Available online at www.sciencedirect.com
ScienceDirect
Ceramics International 37 (2011) 2549–2553
CERAMICS INTERNATIONAL
www.elsevier.com/locate/ceramint

Fabrication of bulk macroporous zirconia by combining sol–gel with calcination processes

Zijun Zhang, Jiurong Liu *, Fenglong Wang, Jing Kong, Xinzhen Wang

Key Laboratory for Liquid–Solid Structural Evolution and Processing of Materials, Ministry of Education and School of Materials Science and Engineering, Shandong University, Jinan, Shandong 250061, People's Republic of China

Received 22 February 2011; received in revised form 31 March 2011; accepted 31 March 2011
Available online 7 April 2011

Abstract

Macroporous yttria-stablized tetragonal zirconia has been synthesized combining the sol–gel with Pechini method. Polyacetylacetonatozirconium (PAZ) served as the zirconium precursor while polyvinyl alcohol (PVA) was used as pore template. The thermal behaviors of xerogel and porous zirconia were determined by thermogravimetric/differential thermal analysis (TG/DTA). FT-IR, FE-SEM, and XRD analysis indicated that the organic components of xerogel have been completely removed and porous zirconia was formed after annealing at 600 °C for 2 h in air. The skeleton is composed of zirconia particles with diameter of about 60 nm and the pore diameter is about 68 nm. The surface area and pore volume of the bulk macroporous yttria-stablized tetragonal zirconia are 9.4 m^2/g and 0.016 cm^3/g, respectively, evaluated from nitrogen adsorption/desorption measurements.

Keywords: Sol–gel; Macroporous; Zirconia xerogel; PAZ; Thermal behavior

1. Introduction

Zirconia has received much attention due to its important applications in gas sensors [1], catalysts supports [2,3], solid oxide fuel cells [4,5], biological materials [6,7], ceramic filter and thermal barrier [8–10]. The researches of porous zirconia materials are gradually considered to be more important since the performance of zirconia materials depends not only on the chemical composition and morphology, but also greatly on surface area and pore characteristics. Zirconia porous materials with tailored morphology, e.g., powder, film, and fiber, have been widely studied for various practical applications [11–16]. However, few contributions have been presented for fabricating bulk zirconia porous materials, which will be more useful in the applications of catalysts supports, solid oxide fuel cells, ceramic filter and thermal barrier. It is well known that ZrO_2 containing more than 8 mol% Y_2O_3 stabilized the cubic phase at room temperature, while 3 mol% Y_2O_3 doped ZrO_2 is tetragonal phase. When the doping amount of Y_2O_3 is between 3 mol% and 8 mol%, a mixture of tetragonal and cubic phase will be obtained [17,18].

In order to obtain yttria-stabilized porous zirconia materials with chemical homogeneity and nanometric dimensions, various techniques including solid state reaction process [19], sol–gel method [20–22], tape casting [23], hydrothermal treatments [24,25], thermal decomposition [26] and polymeric routes [27,28] have been investigated. The Pechini method provides a chemical route to distribute metal ions uniformly in polymer or resin network at atomic scale [29–31]. The sol–gel process is appropriate to fabricate powders with controllable porosity since it provides not only good homogeneity of different precursors but also better control of grain size and pore distribution [3,32]. In the present study, bulk yttria-stabilized tetragonal zirconia porous materials were prepared via a revised sol–gel route combining sol–gel process with Pechini method, in which polyacetylacetonatozirconium (PAZ) was used as the precursor to provide Zr^{4+} ion and polyvinyl alcohol (PVA) was added as pore template. The formations of sol–gel, decomposition of xerogel, and crystallization of zirconia have been investigated by DTA, FT-IR, and XRD analysis. The morphology and porosity of final product were also studied through SEM and nitrogen adsorption/desorption measurements.

* Corresponding author. Tel.: +86 0531 8839 2036; fax: +86 0531 8839 2315.
E-mail address: jrliu@sdu.edu.cn (J. Liu).

0272-8842/$36.00
doi:10.1016/j.ceramint.2011.03.054

2. Experimental

2.1. Preparation of zirconia xerogel

The precursor PAZ (polyacetylacetonatozirconium) was synthesized according to the procedure described in the previous reports [33–35]. The experimental processes are depicted schematically in Fig. 1. In a typical process, 4.3 g PAZ and 6 mol% yttrium nitrate as phase stabilizer were dissolved in 15 ml deionized water to form solution. 0.5 g PVA was dissolved in 15 ml deionized water at 80 °C under magnetic stirring. After cooled to room temperature, the PVA solution was added into PAZ and yttrium nitrate solution to obtain a viscous sol solution after magnetic stirring for 2 h, and then the solution was transferred into a vessel. The xerogel was obtained after the sol solution was aged and dried at 60 °C for 100 h in an oven.

2.2. Fabrication of macroporous zirconia

Prior to calcination, the xerogel was heated to 200 °C for 4 h to remove the absorbed water. The porous yttria-stabilized zirconia (YSZ) bulk sample was obtained after the xerogel was calcined at 600 °C for 2 h in air at a ramp rate of 10 °C min^{-1} in a furnace to remove polymer PVA and acetylacetone ligand.

2.3. Thermal analysis

The thermal decomposition characteristics of the xerogel were measured by thermogravimetric/differential thermal analysis that is conducted on a diamond TG/DTA Perkin Elmer instrument at a heating rate of 10 °C min^{-1} under air flux.

2.4. FT-IR measurements

The Fourier-transformed infrared spectroscopy (FT-IR) was performed with a Thermo-Nicolet Avatar 370 infrared spectrometer in an IR detection range of 400–4000 cm^{-1}.

2.5. FE-SEM and XRD characteristics

The microstructures of resultant products were examined by using a JSM-6700F field emission scanning electron microscope (FE-SEM) at an accelerating voltage of 20 kV and electric current of 1.0×10^{-10} Å. The crystalline phases were characterized by a Rigaku Dmax-rc X-ray diffractometer (XRD) with Ni ltered Cu Kα radiation (V = 40 kV, I = 50 mA) at a scanning rate of 4°/min.

2.6. N_2 adsorption/desorption measurements

The N_2 adsorption/desorption isotherms of the bulk porous zirconia sample were measured at 77 K on a Quadrasorb-SI instrument. The specific surface area was calculated by N_2 physisorption (S_{BET}) and the pore size distribution was calculated by the density functional theory (DFT) method.

3. Results and discussion

3.1. Thermal behavior

From the optical photograph as shown in Fig. 2, the xerogel is observed to be transparent and remains intact after aging and drying process in addition to slightly shrinkage in size due to

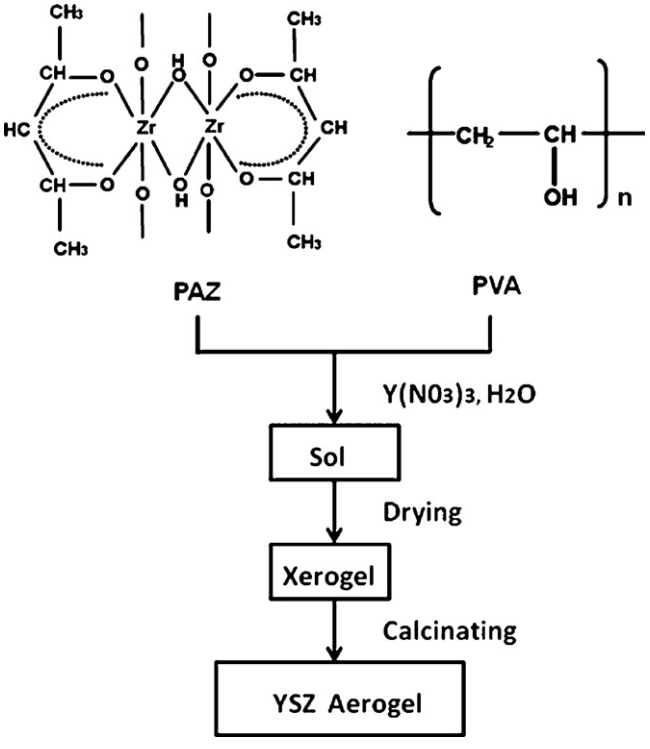

Fig. 1. Schematic diagrams illustrating the synthesis of bulk macroporous zirconia.

Fig. 2. Optical photograph of zirconia xerogel after aging and drying at 60 °C for 100 h.

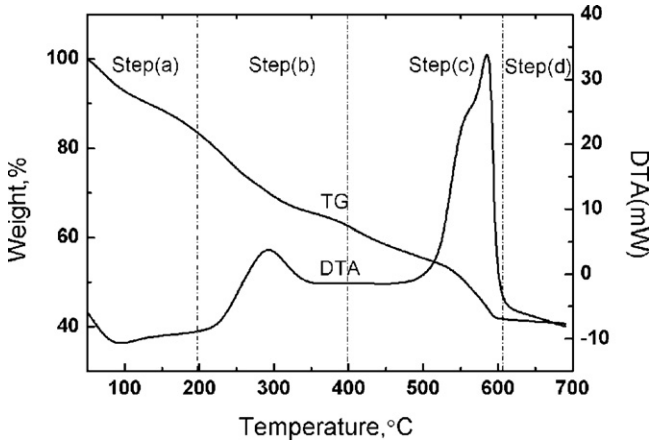

Fig. 3. TG/DTA curves of zirconia xerogel at a heating rate of 10 °C min^{-1} under air flux.

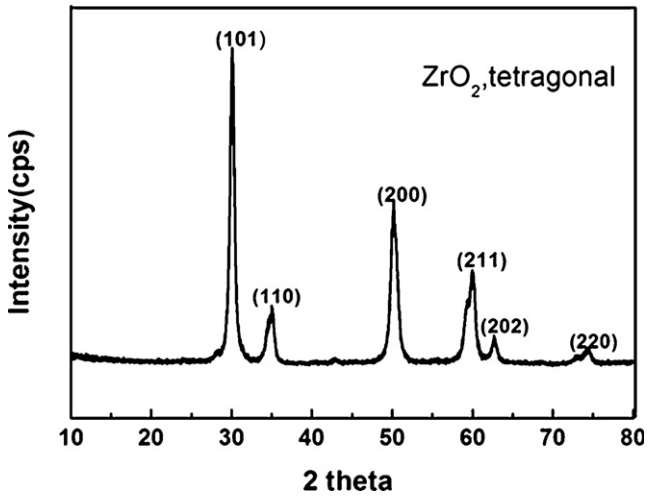

Fig. 5. X-ray diffraction pattern of 3 mol% yttria-stabilized macroporous zirconia sintered at 600 °C for 2 h in air.

the evaporation of solution. Fig. 3 shows the results of TG/DTA analysis for the xerogel sample. Dehydration, oxidation, and crystallization occurred in the calcination process [36] with around 58% weight loss. Based on the analysis of TG and DTA, the calcination process can be subdivided into four steps. In step (a), from the room temperature to 200 °C, the weight loss was about 16% corresponding to the desorption of physically absorbed solvent in the gel. In step (b), an exothermic peak at 200–400 °C observed in the DTA curve accompanying with the intensive 22% weight loss in the TG curve is attributed to the bond breaking and oxidative decomposition of organic components in PAZ precursor and PVA polymer to form volatile species such as CO, CO_2 and H_2O, which result in the removal of organic materials. In step (c) (400–610 °C), the maximum exothermic peak detected in DTA curve with 20% weight loss is mainly attributed to the combustion of organic residues and the dehydroxylation of Zr–OH to form ZrO_2 cyrstallines [29]. In the temperature range of 610–680 °C, there is no apparent exothermal peak and weight loss, suggesting the complete decomposition of organic components.

3.2. FE-SEM and XRD results

Fig. 4 shows the FE-SEM images of 3 mol% Y_2O_3 stabilized zirconia samples. It is demonstrated that, with controlled PVA amount, the wormhole-like zirconia has been prepared. Close inspection reveals that the zirconia particles with diameter of about 60 nm cohered together to form the skeleton in the calcination process and the pore diameter is about 70 nm. The formation mechanism of the macroporous zirconia can be understood as follows: Firstly, the precursor (PAZ) and the polymer (PVA) were dissolved in water homogeneously to form sol solution. The bulk xerogel was obtained after the sol solution was aged and dried in a vessel at 60 °C for 100 h. With subsequent calcination at 600 °C for 2 h in air, PAZ precursor was oxidized to form zirconia skeleton, and polymer PVA and solvent were removed to generate the pores. As a result, the porous zirconia with three-dimensional network architecture was obtained. The phase and purity of the porous zirconia was investigated by XRD. As shown in Fig. 5, all peaks could be indexed as the tetragonal zirconia (JCPDS card No.42-1164), and no peak of any other phase is detected indicating that Y_2O_3 as phase stabilizer was incorporated into the crystalline lattice of tetragonal zirconia in the calcination process [37].

3.3. Characteristics of IR

To complement the XRD and TG/DTA analysis, FT-IR was performed for the zirconnia xerogel and porous zirconnia in an

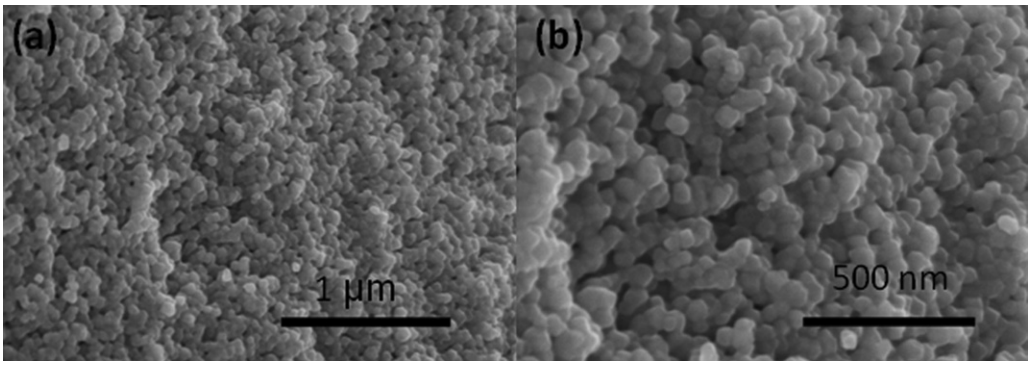

Fig. 4. FE-SEM photographs (a and b) for 3 mol% yttria-stabilized macroporous zirconia sintered at 600 °C for 2 h in air.

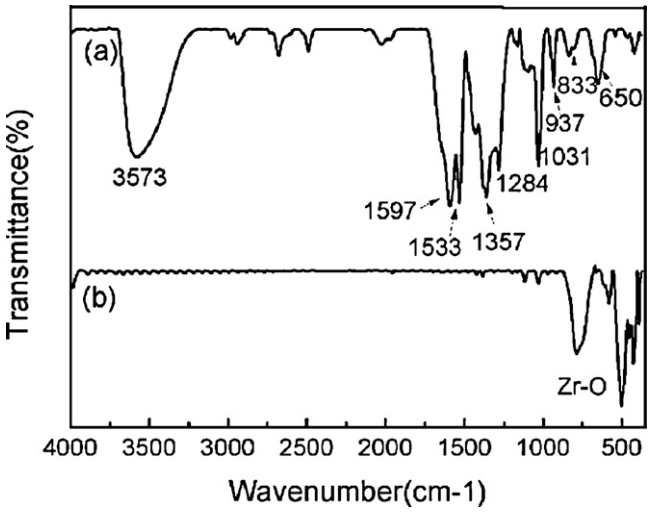

Fig. 6. FT-IR spectra of yttria-stabilized zirconia xerogel (a) and macroporous structure (b).

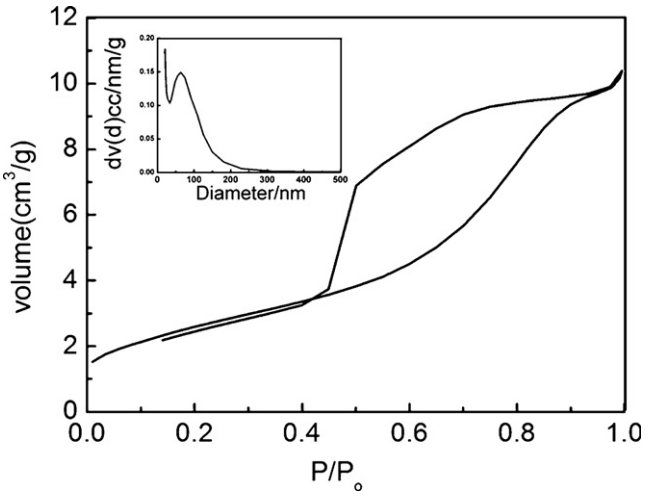

Fig. 7. The nitrogen adsorption/desorption isotherms and the pore size distribution (inset) for 3 mol% yttria-stabilized macroporous zirconia sintered at 600 °C for 2 h in air.

IR detection range of 400–4000 cm^{-1}. In Fig. 6(a), the FT-IR spectra of zirconia xerogel showed that a broad peak at 3573 cm^{-1} was assigned to O-H stretching mode, and the peaks between 2800 cm^{-1} and 3000 cm^{-1} are attributed to the C-H stretching modes. The bands around 1597 cm^{-1} and 1533 cm^{-1} could be assigned to the metal bonded C–O vibration mode of acetylacetone group in PAZ [38,39]. The peaks at 1357 cm^{-1}, 1284 cm^{-1} and 1031 cm^{-1} are attributed to the C–C bonds. The bands at 937 cm^{-1}, 833 cm^{-1} and 650 cm^{-1} are characteristics of Zr–O bonds forming bridges in a ring structure of PAZ (shown in Fig. 1) [35]. After annealing at 600 °C for 2 h, all of the organic species were completely removed, forming the porous zirconia. The FT-IR measurement [Fig. 6(b)] confirmed the complete removal of organic components based on the disappearance of the C–H (2939 cm^{-1}), C–O (1597 and 1533 cm^{-1}), and C–C (1357, 1284, and 1031 cm^{-1}) vibration modes. The C and H elements were likely to react with oxygen to form volatile species such as CO, CO_2, and H_2O, which resulted in the removal of organic species. Moreover, the bands associated with the vibration mode of O–Zr–O bonds of ZrO_2 appeared in 400–500 cm^{-1} as shown in Fig. 6(b). The FT-IR analysis indicated that the organic species of xerogel have been removed and zirconia was formed after annealing, which are in good agreement with the results of XRD and TG/DTA measurements.

3.4. Surface area and pore size distribution

As shown in Fig. 7, the nitrogen adsorption/desorption isotherms indicate that the isotherms of macroporous zirconia sintered at 600 °C are typically IV type with large hysteresis loops [40,41]. This kind of hysteresis results from the capillary condensation associated with large pore channels, which agree with the FE-SEM observation of porous zirconia sample [38]. The specific surface area of the obtained macroporous zirconia is 9.4 m^2/g, and the pore volume is about 0.016 cm^3/g. The corresponding pore size distribution is quite narrow with pore radii about 68 nm (inset), consistent with FE-SEM results. In order to adjust the pore volume of bulk porous zirconia, we also carried out a series of experiments by varying the addition quantity of pore template (PVA) while the other experimental parameters were kept. Experimental results indicated that the pore volume increased with increasing the addition quantity of PVA. However, when 0.6 g PVA was added into the sol solution, the bulk porous zirconia was cracked after calcinations due to the collapse of zirconia skeleton.

4. Conclusions

Polyacetylacetonatozirconium (PAZ) was used as zirconium precursor and polymer PVA was added as pore template to prepare bulk macroporous zirconia by a revised sol–gel method. Porous zirconia with three-dimensional network architecture was obtained after a calcination process, in which PAZ precursor was oxidized to form zirconia skeleton, and polymer PVA and solvent were removed to generate the pores. 3 mol% Y_2O_3 doped into zirconia stabilized the tetragonal phase at room temperature. The obtained bulk macroporous zirconia has surface area of 9.4 m^2/g and pore volume of 0.016 cm^3/g. This study provides a new feasible method to prepare bulk macroporous zirconia, which has potential applications in catalysts supports, solid oxide fuel cells, ceramic filter and thermal barrier.

Acknowledgements

This work was supported by the grant for Qi-Lu Young Scholar program and the Independent Innovation Foundation of Shandong University (2009JQ015). The authors also acknowledge the financial supports from the Research Fund for the Doctoral Program of Higher Education of China (20090131120032), the Excellent Young Scientist Fund of Shandong Province (BS2009CL040) and the Returned Overseas Chinese Scholars, State Education Ministry.

References

[1] G. Korotcenkov, S.D. Han, J.R. Stetter, Review of electrochemical hydrogen sensors, Chem. Rev. 109 (2009) 1402–1433.

[2] J. Goscianska, M. Ziolek, E. Gibson, M. Daturi, Meso-macroporous zirconia modified with niobium as support for platinum acidic and basic properties, Catal. Today 152 (2010) 33–41.

[3] D.A. Ward, E.I. Ko, Preparing catalytic materials by the sol–gel method, Ind. Eng. Chem. Res. 34 (1995) 421–433.

[4] S.P.S. Badwal, F.T. Ciacchi, V. Zelizko, K. Giampietro, Oxygen removal and level control with zirconia – yttria membrane cells, Ionics 9 (2003) 315–320.

[5] E.C. Sbuarao, H.S. Maiti, Solid electrolytes with oxygen ion conduction, Solid State Ionics 11 (1984) 317–338.

[6] R. Fan, Y. Huh, Y. Yan, J. Arnold, P. Yang, Gated proton transport in aligned mesoporous silica films, Nat. Mater. 7 (2008) 524–531.

[7] Y.Q. Wang, G. Sayre, Commercial thermal barrier coatings with a double-layer bond coat on turbine vanes and the process repeatability, Surf. Coat. Technol. 203 (2009) 2186–2192.

[8] C. Viazzi, J.P. Bonino, F. Ansart, Synthesis by sol–gel route and characterization of yttria stabilized zirconia coatings for thermal barrier applications, Surf. Coat. Technol. 201 (2006) 3889–3893.

[9] A.D. Mazzoni, M.S. Conconi, Study of carbonitriding reactions of zirconia. synthesis of Zr(C,N,O) phases and β-type zirconium oxynitrides, Ceram. Inter. 30 (2004) 23–29.

[10] K.S. Ravichandran, K. An, R.E. Dutton, S.L. Semiatin, Thermal conductivity of plasma-sprayed monolithic and multilayer coatings of alumina and yttria-stabilized zirconia, J. Am. Ceram. Soc. 82 (1999) 673–682.

[11] J. Tulliania, C. Bartuli, E. Bemporad, V. Naglieri, M. Sebastiani, Preparation and mechanical characterization of dense and porous zirconia produced by gel casting with gelatin as a gelling agent, Ceram. Inter. 35 (2009) 2481–2491.

[12] K. Cassiers, T. Linssen, K. Aerts, P. Cool, O. Lebedev, G.V. Tndeloo, R.V. Grieken, E.F. Vansant, Controlled formation of amine-templated mesostructured zirconia with remarkably high thermal stability, J. Mater. Chem. 13 (2003) 3033–3039.

[13] E.L. Crepaldi, G. Soler-Illia, D. Grosso, P.A. Albouy, C. Sanchez, Design and post-functionalisation of ordered mesoporous zirconia thin films, Chem. Commun. 17 (2001) 1582–1583.

[14] G. Yu, L. Zhu, X. Wang, H. Chen, G. Zhang, Z. Sun, H. Fan, X. Liu, D. Xu, Fabrication of zirconia mesoporous fibers by using polyorganozirconium compound as precursor, Micropor. Mesopor. Mater. 119 (2009) 230–236.

[15] S.H. Hakim, B.H. Shanks, A comparative study of macroporous metal oxides synthesized via a unified approach, Chem. Mater. 21 (2009) 2027–2038.

[16] W. Stichert, F. Schuth, Influence of crystallite size on the properties of zirconia, Chem. Mater. 10 (1998) 2020–2026.

[17] J. Chavalier, L.T. Gremillard, The tetragonal-monoclinic transformation in zirconia: lessons learned and future trends, J. Am. Ceram. Soc. 92 (2009) 1901–1920.

[18] E.C. Grzebielucka, A.S.A. Chinelatto, S.M. Tebcherani, A.L. Chinelatto, Synthesis and sintering of Y_2O_3-doped ZrO_2 powders using two Pechini-type gel routes, Ceram. Inter. 36 (2010) 1737–1742.

[19] V.V. Mishra, A.K. Garg, D.C. Agrawal, Preparation of tetragonal zirconia powders by a solid state reaction: kinetics, phases and morphology, Bull. Mater. Sci. 21 (1998) 81–86.

[20] C.N. Chervin, B.J. Clapsaddle, H.W. Chiu, A.E. Gash, J.H. Satcher, S.M. Kauzlarich, Aerogel synthesis of yttria-stabilized zirconia by a non-alkoxide sol–gel route, Chem. Mater. 17 (2005) 3345–3351.

[21] V. Vladimir, R.P. Omorjan, Electrical conductivity of sol–gel derived yttria-stabilized zirconia, Ceram. Inter. 27 (2001) 859–863.

[22] S. Shukla, S. Seal, Effect of HPC and water concentration on the evolution of size, aggregation and crystallization of sol–gel nano zirconia, J. Nanoparticle Res. 4 (2002) 553–559.

[23] P.G. McCormick, T. Tsuzuki, J.S. Robinson, J. Ding, Nanopowders synthesized by mechanochemical processing, Adv. Mater. 13 (2001) 1008–1010.

[24] E. Hemmer, K. Soga, T. Konishi, T. Watanabe, T. Taniguchi, S. Mathur, Influence of the host phase on the vibrational spectra of europium-doped zirconia prepared by hydrothermal processing, J. Am. Ceram. Soc. 93 (2010) 3873–3879.

[25] A. Ahniyaz, T. Watanabe, M. Yoshimura, Tetragonal nanocrystals from the $Zr_{0.5}Ce_{0.5}O_2$ solid solution by hydrothermal method, J. Physic. Chem. B 109 (2005) 6136–6139.

[26] B. Xia, I.W. Lenggoro, K. Okuyama, Novel route to nanoparticle synthesis by salt-assisted aerosol decomposition, Adv. Mater. 13 (2001) 1579–1582.

[27] S.S. Pathak, I.C. Pius, R.D. Bhanushali, T.V.V. Rao, S.K. Mukerjee, Preparation of porous zirconia microspheres by internal gelation method, Mater. Res. Bull. 43 (2008) 2937–2945.

[28] S. Farhikhteh, A. Maghsoudipour, B. Raissi, Synthesis of nanocrystalline YSZ (ZrO_2–$8Y_2O_3$) powder by polymerized complex method, J. Alloy Comp. 491 (2010) 402–405.

[29] J.H. Schattka, D.G. Shchukin, J. Jia, M. Antonietti, R.A. Caruso, Photocatalytic activities of porous titania and titania/zirconia structures formed by using a polymer gel templating, Chem. Mater. 14 (2002) 5103–5108.

[30] J.O. Landeros, M.E.C. Garcia, H. Pfeiffer, Synthesis of macroporous ZrO_2–Al_2O_3 mixed oxides with mesoporous walls, using polystyrene spheres as template, J. Porous Mater. 16 (2009) 473–479.

[31] B. Smarsly, S. Polarz, M. Antonietti, Preparation of porous silica materials via sol–gel nanocasting of nonionic surfactants: a mechanistic study on the self-aggregation of amphiphiles for the precise prediction of the mesopore size, J. Phys. Chem. B 105 (2001) 10473–10483.

[32] W. David, I.K. Edmond, Preparing catalytic materials by the sol–gel method, Ind. Eng. Chem. Res. 34 (1995) 421–433.

[33] G. Yu, L. Zhu, X. Wang, J. Liu, D. Xu, Fabrication of silica-supported ZrO_2 mesoporous bers with high thermal stability by sol–gel method through a controlled hydrolysis-condensation process, Micropor. Mesopor. Mater. 130 (2010) 189–196.

[34] M. Pan, J. Liu, M. Lu, D. Xu, D. Yuan, D. Chen, P. Yang, Z. Yang, Preparation of zirconia xerogels and ceramics by sol–gel method and the analysis of their thermal behavior, Thermochim. Acta 376 (2001) 77–82.

[35] L. Zhu, G. Yu, X. Wang, X. Hou, X. Liu, J. Sun, Z. Sun, H. Fan, D. Xu, Thermal behavior of polyacetylacetonatozirconium (PAZ), Thermochim. Acta 473 (2008) 81–85.

[36] R.S. Silva, M.L. Bernardino, A.C. Hernandes, Synthesis of non-agglomerated $Ba_{0.77}Ca_{0.23}TiO_3$nanopowders by a modified polymeric precursor method, Sol–gel Sci. Technol. 42 (2007) 173–179.

[37] M. Mamak, N. Coombs, G. Ozin, Self-assembling solid oxide fuel cell materials: mesoporous yttria-zirconia and metal-yttria-zirconia solid solutions, J. Am. Chem. Soc. 122 (2000) 8932–8939.

[38] S. Masoud, M. Dadkhah, F. Davar, Pure cubic ZrO_2 nanoparticles by thermolysis of a new precursor, Polyhedron 28 (2009) 3005–3009.

[39] J. Liu, Y. Mao, E. Lan, D.R. Banatao, G.J. Forse, J. Lu, H.O. Blom, T.O. Yeates, B. Dunn, J.P. Chang, Generation of oxide nanopatterns by combining self-assembly of s-layer proteins and area-selective atomic layer deposition, J. Am. Chem. Soc. 130 (2008) 16908–16913.

[40] J.W. Kriesel, M.S. Sander, T.D. Tilley, Block copolymer-assisted synthesis of mesoporous, multicomponent oxides by nonhydrolytic, thermolytic decomposition of molecular precursors in nonpolar media, Chem. Mater. 13 (2001) 3554–3563.

[41] A. Pattanayak, A. Subramanian, Production of meso- and giga-porous zirconia particles—an improved multi-step particle aggregation process, Powder Technol. 192 (2009) 359–366.